SUPPLEMENTARY INFORMATION

SUPPLEMENTARY TEXT

ANALYSIS OF BR1

Superimposition of the ^{1}H-^{15}N HSQC spectra of the free protein with the (1:1) [Δ–Cter SmpB/TLD60] complex: as observed before (*1*), the addition of TLD60 yields line-broadenings and disappearances of several cross-peaks, characteristic of the intermediate exchange regime between the free and the bound states. Nevertheless, most resonances were assigned by comparison to the reference spectrum of the free protein indicating that the overall structure of the protein is retained in the complex, despite local changes (supporting Fig. S2). Upon adding the TLD60, the changes are clustered around beta sheet 1 (D5-I8), from beta sheet 2 to helix alpha 2 (T25-K33 and E36-G44), in beta sheets 4 (A60-L62) and 5 and at the top of helix alpha 3 (K85-L96). All these residues form a binding domain called « Binding Region 1 » (BR1). Most residues from BR1 are identical in the two SmpB sequences from *T. thermophilus* and *A. aeolicus* (T25-I30, L32, K33, E36-R41, G44, position 61 is an aromatic, L62, K85 and L86). Most of them are well conserved among bacteria (*2*). SmpB from these two bacteria adopt similar 3D structures (*1,3*). As for the SmpB/complex in *T. thermophilus* (*1*), important changes including the disappearance of several peaks were observed. It concerns residues E27, G29, V31, K33, E56, G58, K85 and N117 in *A. aeolicus*, the respective counterparts of E21, G23, A25, K27, E49, G51, K78 and G111 in *T. thermophilus*. Our results are also consistent with the crystal structure of the complex in which residues from BR1 either interact with the tRNA domain of tmRNA or are located on the interacting surface (*2*). Backbone amide resonances of R41 and V37 (helix alpha 2) disappear and those of W114 (beta sheet 6) undergo substantial shifts. Large broadenings and frequency shifts are seen on more than one third of the amino acids of the flexible central loop 2. Y70, which corresponds to Y63 in *T. thermophilus*, interacts with guanine G49 in the TLD T-stem, as well as on the very conserved and solvent exposed residues of beta sheet 5, located in the vicinity of the variable arm of tmRNA in the crystallographic complex (*2*). Altogether, our results are in agreement with both the earlier crystallographic (*2,4*) and NMR (*1,5*) structural data published for the [TLD/SmpB] complex in Thermophiles. Our results also confirm that TLD binding to BR1 induces conformational changes around alpha 1 and the truncated C-terminal region (E15, A18, G128, L131 and D133), far from the main interacting area. The use the [Δ–Cter SmpB/TLD60] complex is thus validated to probe the interactions of the TLD-SmpB complex with the decoding site of stalled ribosomes.

SUPPLEMENTARY METHODS

The SmpB and DC sequences for the NMR. To compare with published data (2-4,6), we worked with the *A. aeolicus* version of SmpB and with an RNA mimicking an *E. coli* DC. Its NMR structure was solved with antibiotics (7). The sequence of the *A. aeolicus* DC is identical to that of *E. coli* except for the G1410-C1490 pair replacing A1410-U1490. We worked with SmpB deleted from its 17 C-terminal residues because: i) the C-term tail is dispensable for the recruitment of tmRNA to the ribosomes, ii) the chemical probing of the 16S rRNA in the presence of SmpB indicates that the C-tail protects G530 from chemical modifications (absent from the small DC) without inducing reactivity changes at A1492 and A1493, iii) its absence reduces protein aggregation in the presence of the RNA. The system studied is composed of the Δ–Cter SmpB, the 60-mer TLD RNA mimic

(TLD60) and either a 27 or a 33 nt-long RNA (DC27 and DC33, Fig. 3a). TLD60 contains T54 and Ψ55 (8). Its structure is stable and homogeneous (8. The sequence of DC33 is identical to that of DC27 except for 3 extra GC pairs stabilizing the two ends.

NMR Titration and Chemical Shift Perturbations Mapping. All titrations were performed at 313K. The sample volumes were readjusted at each step to their initial value by lyophilization. HSQC spectra were recorded after a 1-hour equilibration at 313K in the spectrometer. Titration of BR1 was conducted by recording four ^{1}H, ^{15}N HSQC spectra of ^{15}N Δ–Cter SmpB upon addition of TLD60 at the molar ratios of 0.2, 0.5, 1 and 2. The mixture was then readjusted to equimolar concentration by addition of ^{15}N-Δ–Cter SmpB and checked by running an extra ^{1}H-^{15}N HSQC experiment. For the second stage (titration of BR2), aliquots of a stock solution of DC27 (0.2mM) were added to the (1:1) [^{15}N-Δ–Cter SmpB/TLD60] complex. Five points were recorded at molar ratios of 0.4, 1, 4.5 and 8. The changes in the chemical shifts of the amide ^{1}H and ^{15}N were averaged by using the formula: $wacs = \{[1/2[(\Delta H)^2 + (0.2\Delta N)^2]]\}^{1/2}$ (12-14) and plotted versus the residue number. The cutoff value (c.o.) of $\square+\sigma$ was computed. All residues undergoing wacs > c.o. were mapped in red on the ribbon structure, and those with wacs in the ranges [c.o. - 90% c.o] and [90% c.o. - 80% c.o.] respectively in orange and yellow. Amino acids with NH cross-peak broadened to baseline were mapped in magenta. The reciprocal titration was run in D_2O buffer by adding 0.2, 1, 2 and 3 eq. of a stock solution of the unlabeled (1:1) [Δ–Cter SmpB/TLD60] to a 0.2mM solution of ^{13}C,^{15}N-DC33. The titration was monitored by recording ^{1}H-^{13}C HSQC spectra, and following the aromatic C2H2 and C8H8 cross-peaks chemical shift variations.

Docking procedures of the SmpB-TLD complex within the ribosome

We started with the structure of the ribosome (PDB 2j00 and 2j01). Full-length A-site tRNA (PDB 1GIX, 9) was docked into the A-site, replacing the anticodon stem-loop. The A-site tRNA was replaced by the TLD-SmpB complex (2), by superimposing the TLD acceptor stem and T stem-loop onto that of the tRNA. The T. thermophilus SmpB structure was then replaced by its A. aeolicus homolog, either from free state (3) or from the 'TLD-SmpB' complex (Fig. 4, 4). This was dictated by the absence of parts of the TLD acceptor branch within the electron density map from the A. aeolicus complex and because residues 73-75 (loop 2) are missing from SmpB. Both models are superimposable and account for the NMR constraints and for the probing data, with SmpB filling the space previously occupied by the anticodon stem-loop of the A-site tRNA.

Complementation assays. The complementation assays were performed in *E. coli*, using *E. coli* tmRNA and SmpB molecules. *E. coli ΔsmpB* strains and plasmids used for overexpression of both *E. coli* wt and Δ–Cter SmpBs His-tagged in C-ter (6 His) were previously described (10,11). *E. coli* SmpBs are referred here to as ecSmpBs. Double and triple mutations were introduced in the protein by PCR mutagenesis. The double mutant ecSmpBK131A/K133A (ecSmpB-KK protein) and the triple mutant ecSmpBR19A/E23A/Y24A (ecSmpB-REY protein) were cloned into the pBR322-pS vector containing the promoter of the *smpB* gene (11). Complementation assays with ecSmpB, ecSmpB-REY and ecSmpB-KK proteins were performed by the co-transformation of the *E. coli* Δ*smpB* strain with either the pBR322-pS, pBR322-pS-SmpB, pBR322-pS-smpB-REY or pBR322-pS-smpB-KK plasmids. Transformed cells were grown to mid-logarithmic phase at 37°C, diluted at an A_{600} of 0.01 in an LB broth containing ampicillin and incubated at 45°C. The growth of the transformed cells was monitored by the absorbance at 600 nm.

Determination of the location of tmRNA and SmpB mutants in *E. coli*. *E. coli* strains expressing the various ecSmpB mutants and the procedures to recover fractions S100 (soluble material) and P100 (crude ribosome extract) are described (10). For each fraction (S100 and P100), amounts of RNAs and proteins corresponding to the same number of *E. coli* cells were analyzed by either Northern or Western blotting. Pre-hybridization and hybridization with ^{32}P-labeled DNA oligonucleotides complementary to tmRNA (5' –CGG GTA CGG GTA GGA TCG CAC ACC- 3') were carried out in ExpressHyb according to the protocol (Clontech). EcSmpB proteins were detected by Western blotting using rabbit polyclonal antibodies directed against His-tagged SmpB proteins, followed by chemiluminescence detection (Amersham Biosciences).

SUPPLEMENTARY FIGURES

***Fig. S1*:** Interaction of SmpB with a stalled ribosome in comparison with canonical translation. **(a)** Translating ribosome (small subunit: yellow, large subunit: blue) onto an mRNA (dark blue) with tRNAs into the Exit site (E-site, red), the Peptidyl-tRNA site (P site, orange) and the Aminoacyl-tRNA site (A-site, green) (PDB 2HGP and 2HGQ; (15)). **(b)** Ribosome stalled onto a truncated mRNA, with an empty A-site filled by SmpB (pink, PDB 1p6v, (3)) on the 30S, based on cryo-EM data (5). IMAGIC (16) and CHIMERA (17) softwares were used for the volume conversion and visualization. We thank F. Weiss for his assistance in preparing this figure.

Fig. S2: Complex formation between TLD60 and Δ–Cter SmpB defines binding region 1 (BR1). (**a**) Overlay of the ^{1}H-^{15}N HSQC spectra of Δ–Cter SmpB free (black contours) and bound in presence of an equimolar amount of TLD60 (blue contours). (**b**) Histogram of the per-residue number Weighted Average Chemical Shifts. Blanks underlined by magenta correspond to resonances broadened to baseline upon titration.

***Fig. S3*:** TLD60 binds to SmpB region BR1: Color-coded mapping of the significant perturbations onto the protein solution structure (PDB 1K8H1, (3)) as described in Materials and Methods. TLD60 protects residues from BR1 (circled in grey).

***Fig. S4*:** DC27 binds to Δ–Cter SmpB region BR2. (**a**) Per-residue WACS histogram. (**b**) Mapping of the perturbations onto the structure of SmpB (PDB 1K8H1) using same color as in Fig. S3. The "top" face of SmpB is mostly unaffected by addition of the DC RNA.

Fig. S5: Functional importance of BR2. (**a**) Expression levels of tmRNA, wt ecSmpB and mutants ecSmpB proteins in the S100 and P100 fractions. (**b**) Growth of *E. coli ΔsmpB* strains at 45°C free (red) or complemented by a plasmid expressing either wt ecSmpB (blue), ecSmpB-REY (▲), or ecSmpB-KK (■).

SUPPLEMENTARY REFERENCES

1. Nameki N, Someya T, Okano S, Suemasa R, Kimoto M *et al*. (2005) Interaction analysis between tmRNA and SmpB from *Thermus thermophilus*. *J Biochem*. 138:729-739.
2. Bessho Y, Shibata R, Sekine S, Muruyama K, Higashijima K *et al*. (2007) Structural basis for functional mimicry of long-variable-arm tRNA by transfer-messenger RNA. *PNAS* 104:8293-8298.
3. Dong G, Nowakowski J, Hoffman DW (2002) Structure of small protein B: the protein component of the tmRNA-SmpB system for ribosome rescue. *EMBO J*. 21:1845-1854.
4. Gutmann S., Haebel PW, Metzinger L, Sutter M, Felden B, Ban N (2003) Crystal structure of the transfer-RNA domain of transfer-messenger RNA in complex with SmpB. *Nature* 424:699-703.

5. Gillet R, Kaur S, Li W, Hallier M, Felden B, Frank J (2007) Scaffolding as an organizing principle in trans-translation. J. Biol. Chem. 282:6356-6363.
6. Someya T, Nameki N, Hosoi H, Suzuki S, Hatanaka H, Fujii M, Terada T, Shirouzu M, Inoue Y, Shibata T, Kuramitsu S, Yokoyama S, Kawai G (2003) Solution structure of a tmRNA-binding protein, SmpB, from Thermus thermophilus. FEBS Lett 535: 94-100.
7. Fourmy D, Recht MI, Puglisi JD (1998) Binding of neomycin-class aminoglycoside antibiotics to the A-site of 16 S rRNA. J Mol Biol 277: 347-362
8. Gaudin C, Nonin-Lecomte S, Tisné C, Corvaisier S, Bordeau V, Dardel F, Felden, B (2003) The tRNA-like domains of E coli and A. aeolicus transfer-messenger RNA: structural and functional studies. J Mol Biol 331: 457-471
9. Yusupov M, Yusupova G, Baucom A, Lieberman K, Earnest T, Cate J, Noller H (2001) Crystal Structure of the Ribosome at 5.5 Å Resolution. *Science* **292:** 883-896
10. Hallier M, Ivanova N, Rametti A, Pavlov M, Ehrenberg M, Felden B (2004) Pre-binding of small protein B to a stalled ribosome triggers trans-translation. J. Biol. Chem. 279:25978-25985
11. Hallier M, Desreac J, Felden B (2006) Small protein B interacts with the large and the small subunits of a stalled ribosome during trans-translation. Nucleic Acids Res 34: 1935-43
12. Grzesiek S, Bax A, Clore GM, Gronenborn AM, Hu JS, Kaufman J, Palmer I, Stahl SJ, Wingfield PT (1996) The solution structure of HIV-1 Nef reveals an unexpected fold and permits delineation of the binding surface for the SH3 domain of Hck tyrosine protein kinase. Nat. Struct. Biol. 3:340–345.
13. Garrett DS, Seok YJ, Peterkofsky A, Clore GM, Gronenborn AM (1997) Identification by NMR of the binding surface for the histidine-containing phosphocarrier protein HPr on the N-terminal domain of enzyme I of the Escherichia coli phosphotransferase system. Biochemistry 36:4393–4398.
14. Foster MP, Wuttke DS, Clemens KR, Jahnke W, Radhakrishnan I, Tennant L, Reymond M, Chung J, Wright, PE (1998) Chemical shift as a probe of molecular interfaces: NMR studies of DNA binding by the three amino-terminal zinc finger domains from transcription factor IIIA. J. Biomol. NMR 12:51–71.
15. Yusupova G, Jenner L, Rees B, Moras D, Yusupov M (2006) Structural basis for messenger RNA movement on the ribosome. Nature. 444:391-394.
16. Van Heel M, Harauz G, Orlova EV, Schmidt R, Schatz M (1996) A new generation of the IMAGIC image processing system. J. Struct. Biol. 116:17-24.
17. Pettersen EF, Goddard TD, Huang CC, Couch GS, Greenblatt DM, Meng EC, Ferrin TE (2004) UCSF Chimera a visualization system for exploratory research and analysis. J. Comput. Chem. 25:1605-16012.

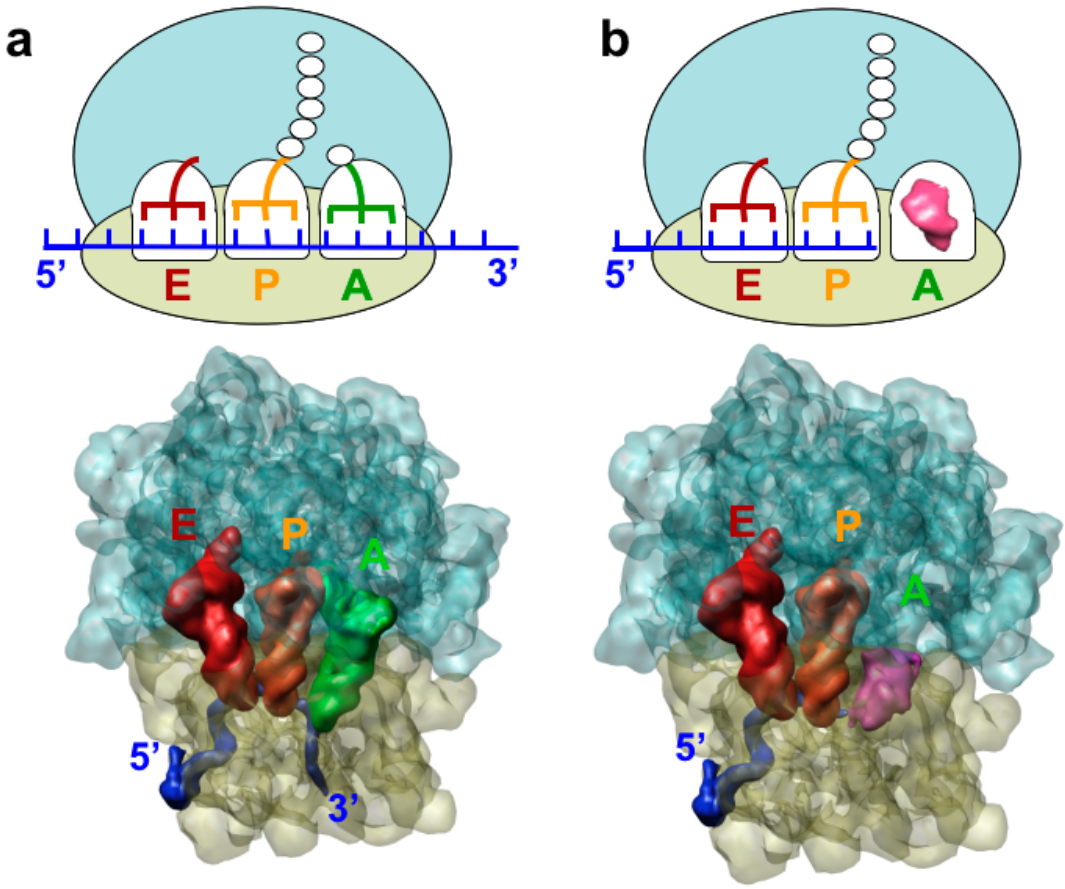

Fig. S1

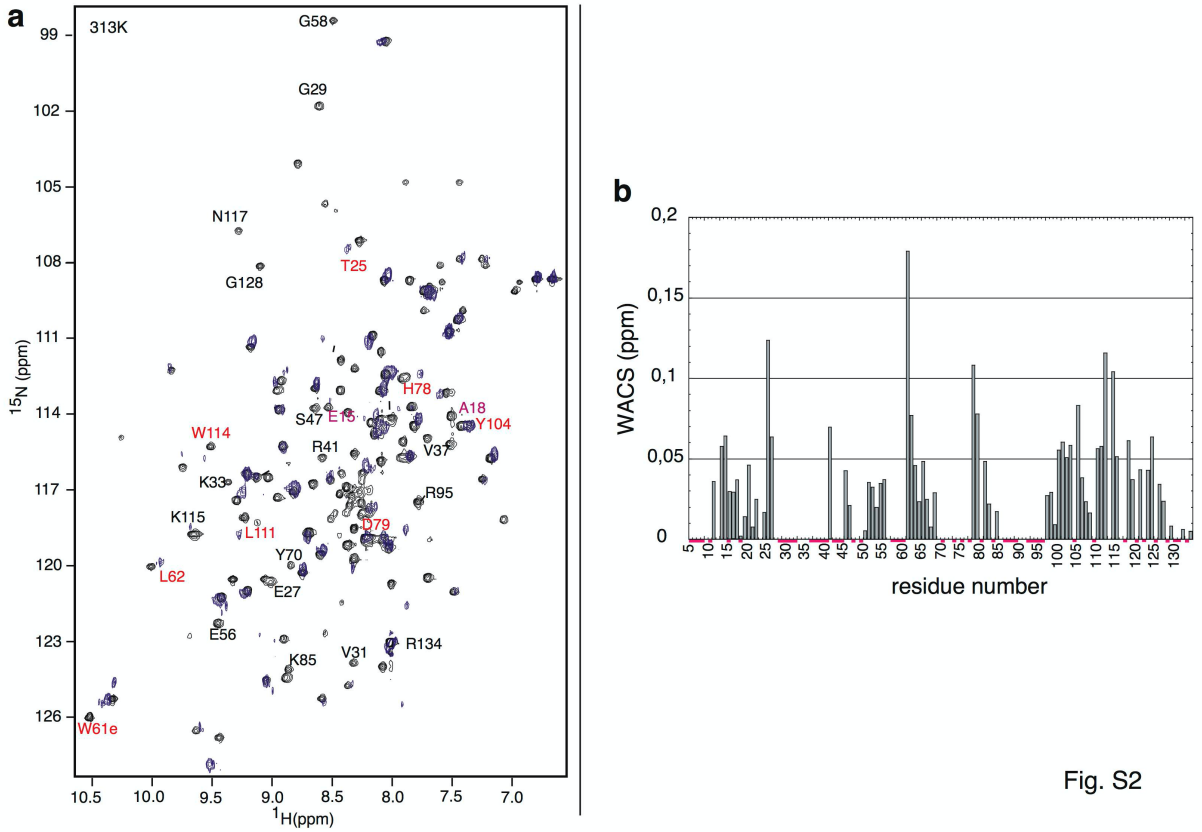
a
313K
G58
G29
N117
T25
G128
H78
A18
Y104
S47
E15
W114
R41
V37
K33
R95
K115
L111
D79
Y70
L62
E27
E56
V31
R134
K85
W61e
99
102
105
108
111
114
117
120
123
126
15N (ppm)
10.5
10.0
9.5
9.0
8.5
8.0
7.5
7.0
1H(ppm)
b
0,2
0,15
0,1
0,05
0
WACS (ppm)
residue number

Fig. S2

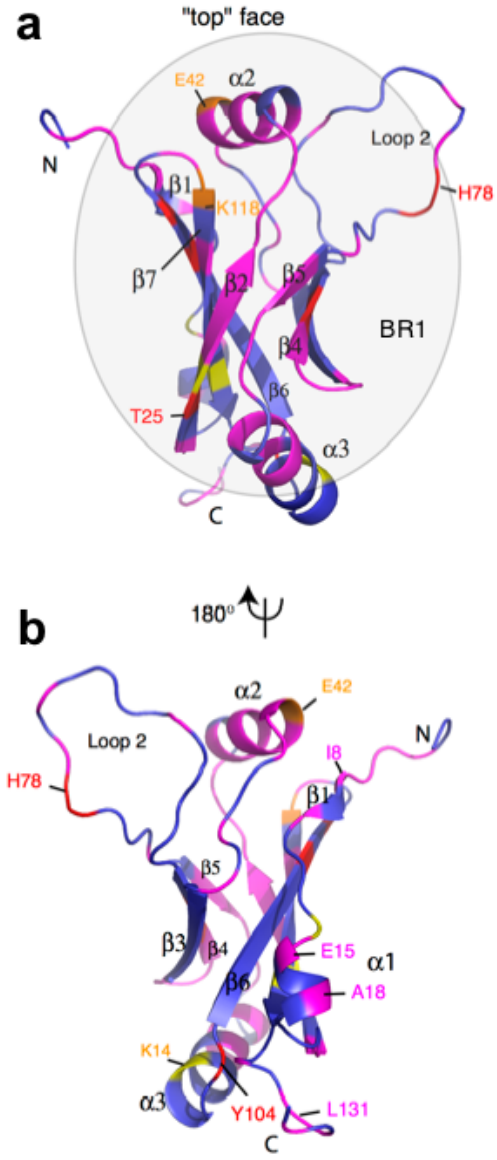
a
"top" face
E42
α2
Loop 2
N
β1
K118
H78
β7
β2
β5
BR1
β4
β6
T25
α3
C
180°
b
α2
E42
Loop 2
N
I8
H78
β1
β5
β3
β4
E15
α1
β6
A18
K14
α3
Y104
L131
C
"bottom" face

Fig. S3

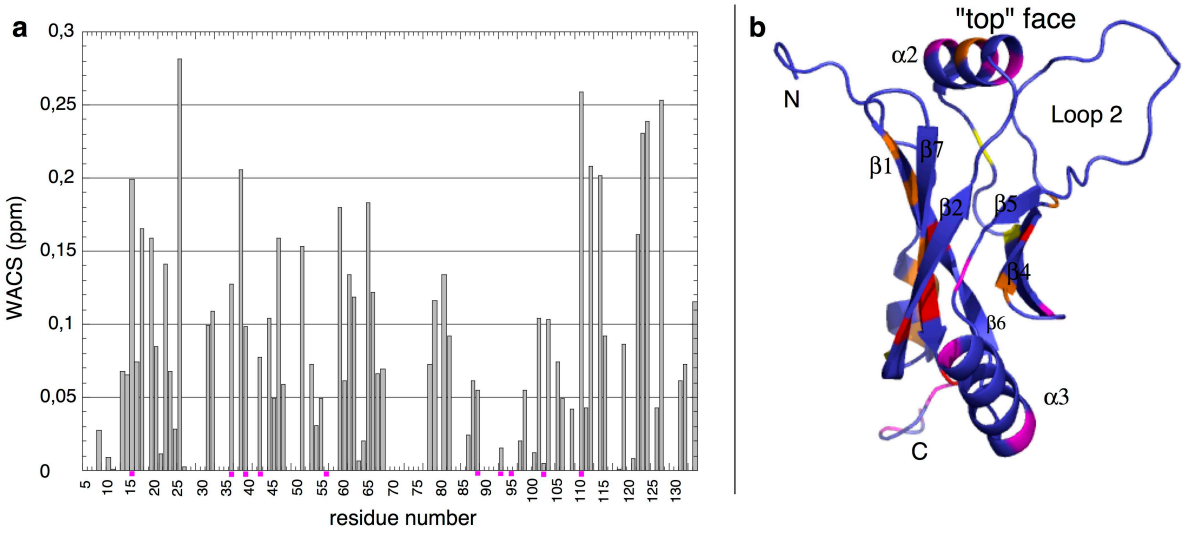
a
WACS (ppm)
residue number
b
"top" face
N
C
Loop 2
α2
α3
β1
β2
β4
β5
β6
β7

Fig. S4

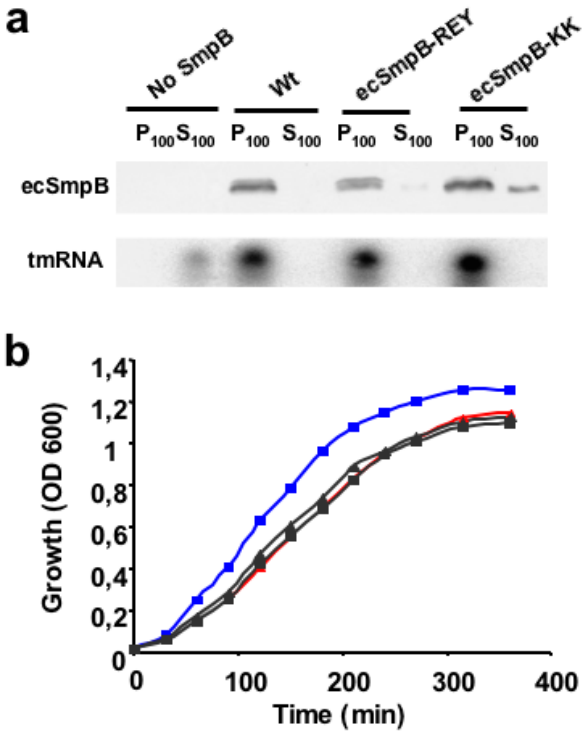
a
No SmpB
Wt
ecSmpB-REY
ecSmpB-KK
P100 S100 P100 S100 P100 S100 P100 S100
ecSmpB
tmRNA
b
Growth (OD 600)
Time (min)

Fig. S5